DOI: 10.61782/fa.2025.0632

NUMERICAL INVESTIGATION ON TONAL NOISE DIRECTIVITY IN DISTRIBUTED PROPULSION SYSTEMS

Alessandro Zarri[1,2]* **Frits de Prenter**[2]

[1] Aeronautics and Aerospace Department, von Karman Institute for Fluid Dynamics, Belgium
[2] Department of Flow Physics and Technology, Delft University of Technology, The Netherlands

ABSTRACT

The potential of distributed electric propulsion to mitigate noise environmental impact has been increasingly explored for UAV and UAM applications. However, when rotors are placed in close proximity, strong aerodynamic interactions and complex acoustic phenomena are induced. Phase synchronization has been proposed as a tonal noise mitigation strategy. Significant reductions in tonal levels have been reported under various configurations, though the extent and nature of such reductions remain debated. Previous assessments have relied on sparse sound pressure measurements, potentially misrepresenting global noise attenuation due to altered directivity. To address this experimental limitation, high-fidelity simulations are carried out for a multi-propeller configuration, focusing on the effects of phase synchronization. The influence of a 30°-phase offset between three co-rotating six-blade rotors is evaluated against an in-phase configuration. A spherical microphone array was used to determine the spatial directivity and total radiated sound power. Results show that phase-angle differences substantially redistribute the acoustic energy toward different spatial locations. Nevertheless, it also impacts the global noise emission, mitigating the sound power level of the opposite-phase configuration by $7.47\,\mathrm{dB}$ in acoustic power for the first BPF harmonic and $4.79\,\mathrm{dB}$ for the second.

Keywords: DEP, propeller noise, aeroacoustics, directivity, phase synchronization

1. INTRODUCTION

The emergence of urban air mobility (UAM) and small-scale unmanned aerial vehicles (UAVs) has spurred interest in novel propulsion systems that reduce environmental impact while improving efficiency. Distributed electric propulsion (DEP) systems, comprising arrays of electrically driven propellers, are promising for enhancing aerodynamic performance and lowering pollutant emissions [1]. When propellers are positioned nearby, as is common in DEP systems, their interactions give rise to complex aerodynamic and acoustic phenomena [2]. These interactions not only affect the aerodynamic loads, leading to increased tonal and broadband noise [3], but also alter the spatial directivity of the blade passing frequency (BPF) harmonics. One proposed method for mitigating such noise is the synchronization of adjacent rotors, typically by imposing a constant phase angle between them. Recently, several studies have investigated the potential of phase synchronization to reduce tonal noise, particularly in hover:

- Pascioni et al. [4] found a 6 dB reduction at the BPF for a 3-bladed, 16-inch propeller at 5100 rpm.
- Shao et al. [5] reported 1–11 dB reductions using 2-bladed, 12-inch propellers at 4000 rpm.
- Guan et al. [6] observed 11–30 dB reductions under hover and low-speed flight (advance ratio 0–0.1) using 2-bladed, 12.5-inch rotors at 6000 rpm.

In forward-flight conditions:

- Turhan et al. [7] measured a 24 dB reduction at the first BPF harmonic with a 90° phase offset between

*Corresponding author: alessandro.zarri@vki.ac.be.

2-bladed propellers.

- De Paola et al. [8] reported a 5 dB reduction using 4-bladed rotors.

These studies suggest that phase synchronization can suppress tonal emissions without compromising thrust, and they often attribute this effect to acoustic interference between the propellers. In contrast to aerodynamic installation effects, which depend on unsteady flow phenomena, acoustic interference stems from phase-coherent sound fields overlapping and interfering destructively or constructively in the far field [9]. However, reported noise reductions vary widely, from 1 dB up to 30 dB for a single-observation microphone. A key limitation of many studies is that only a few microphones are deployed to capture sound pressure levels (SPL) at discrete positions due to limitations in space, time, and cost. Since phase synchronization drastically alters the directivity of tonal components, local SPL measurements may misleadingly suggest strong attenuation, even though sound is merely redirected elsewhere in space. Without capturing the full spatial radiation pattern, it's unclear whether noise is truly reduced or just redistributed. To address this ambiguity, the present study uses high-fidelity numerical simulations to compute the full 3D directivity patterns of DEP systems and to determine the sound power level (SWL), which integrates radiation over all directions. Unlike isolated SPL measurements, SWL offers a global, physically meaningful quantification of noise reduction. This work, therefore, aims to re-evaluate the noise mitigation claims found in the literature by examining the extent to which phase synchronization alters both the directionality and total radiated acoustic power.

2. MATERIALS AND METHODS

2.1 Computational Setup

The simulations replicate the TUD-XPROP-S propeller setup from de Vries et al. [10], involving three six-blade rotors (diameter $D = 0.2032$ m) spaced along the Y-axis, as depicted in Figure 1a. The present work focuses exclusively on two specific phase-synchronized distributed-propulsion configurations, namely with a relative phase angle $\Delta\phi = 0°$ and $\Delta\phi = 30°$, corresponding to the in-phase and opposite-phase rotation, respectively. The simulations analyzed here are the same as those originally introduced in [11] and further extended in [12], to which the reader is referred for additional details on the numerical setup and methodology. The propeller geometry involves a pitch angle of 30° at 70% span and root chord of 16.3 mm, and it was provided by TU Delft. The system rotates anticlockwise with an inflow velocity of $V_\infty = 30$ m/s, and advance ratio $J = 0.8$. The flow around propellers is simulated using SIMULIA PowerFLOW® (version 6-2021-R2), a commercial CFD that employs the Lattice-Boltzmann (LB) method. It solves the LB equation for the particle distribution function $f(\boldsymbol{x}, \boldsymbol{v}, t)$, describing the probability density of particles with velocity $\boldsymbol{v}$ at location $\boldsymbol{x}$ and time t. The simulation uses a D3Q19

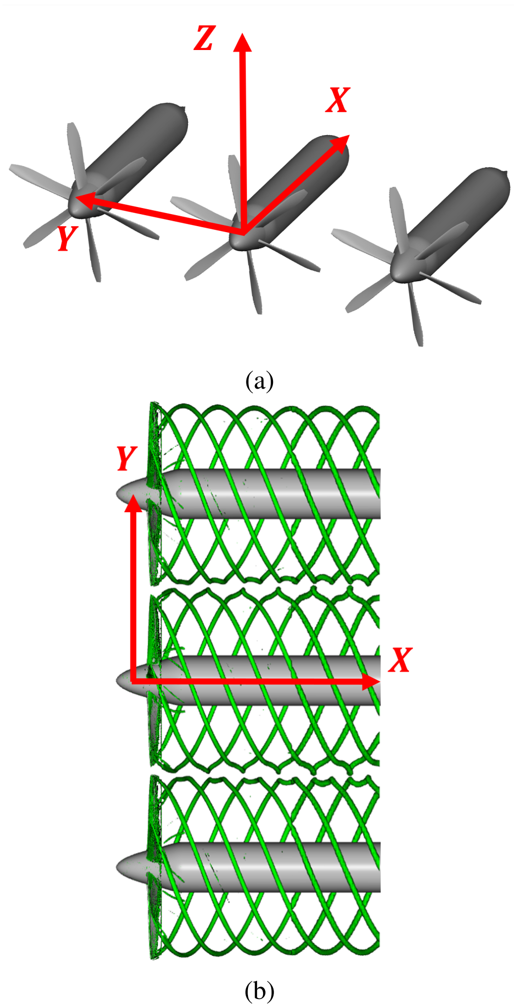

Figure 1: (a) View of the simulated setup with three distributed propellers and the GRS. (b) Visualization of vortex structures with $\lambda 2$ method for the in-phase configuration (b).

stencil for 19 discrete velocity directions and a regularized Bhatnagar-Gross-Krook collision operator. The LB equations are solved on a Cartesian grid with cubic volumetric elements (voxels) and solid objects discretized with planar surface elements (surfels). The solver incorporates a very large eddy simulation (VLES) approach, utilizing a k-ϵ turbulence model. A pressure-gradient extended wall model approximates the no-slip boundary condition. The grid contains approximately 225.5 million voxels, ensuring $y^+ \approx 15$ over the blade surfaces. CPU costs reach roughly 112,000 hours per case. The flow solution can be visualized *via* λ_2 method in Figure 1b.

2.2 Far-Field Noise Computation

The far-field noise formulation used in this work is described and validated in [12]. It exploits the axial and tangential forces computed on the propeller disks as dipole sources radiating sound to the far-field. These forces include the aerodynamic interactions caused by the propellers' proximity. The SPL of the BPF harmonic tones is determined from the measured amplitudes ($p_{\mathrm{BPF_n}}$) using the following equation:

$$L_p(f) = 10 \log_{10} \frac{0.5 p^2_{\mathrm{BPF_n}}}{p^2_{ref}}, \tag{1}$$

which results in the output in acoustic decibels. In this equation, $p_{ref} = 20\,\mu\mathrm{Pa}$ is the reference pressure, while the subscript n indicated the chosen BPF harmonic. For the calculation of the SWL, a spherical microphone array consisting of 2500 microphones is arranged around the propeller at a distance of $100D$ from the global reference system (GRS) origin, ensuring a comprehensive capture of the sound field in all directions. It was confirmed that increasing the number of microphones and the distance from the origin did not affect the SWL. The root mean square (RMS) pressure was computed at all microphone locations. The RMS pressure squared, p^2_{rms}, is the average of the square of the pressure levels at the selected BPF harmonic over all microphone positions. The emitted sound power is then calculated as:

$$\mathrm{W} = p^2_{\mathrm{rms}} A_m / \rho_\infty \, c_\infty, \tag{2}$$

where ρ_∞ is the air density, c_∞ is the speed of sound in air, and the area $A_m = 4\pi R^2_m$ represents the surface area of the sphere formed by the microphone array, with $R_m = 100D$ being the distance from the source to each microphone. Finally, the SWL is computed as:

$$L_w = 10 \log_{10} \left(\frac{\mathrm{W}}{\mathrm{W_{ref}}} \right), \tag{3}$$

where $\mathrm{W_{ref}} = 1 \times 10^{-12}\,\mathrm{W}$ is the reference sound power. This formula yields the SWL in decibels, which quantifies the total acoustic power radiated by the source in all directions.

3. RESULTS

The spatial distribution of sound emissions from a system of three rotors is examined. This distribution is determined by the aerodynamic interaction resulting from the proximity of adjacent propellers, as well as by the interference among the acoustic fields generated by each of the three propellers. In Figure 2a, the $\Delta\phi = 0°$ configuration at the first BPF harmonic is analyzed, and the spatial distribution of the SPL around the propellers' GRS is presented. The SPL mostly contributes around the XY plane and reaches its maximum along the X-axis, with values around $52.7\,\mathrm{dB}$. Along the Y-axis, a lobed pattern is observed, with reduced amplitudes not exceeding $19\,\mathrm{dB}$. In contrast, as shown in Figure 3a for the $\Delta\phi = 30°$ configuration, the directivity pattern of the first BPF harmonic is significantly altered, particularly along the X and Z directions. For instance, if the SPL is measured by a microphone placed along the X-axis, at a distance of $100D$ from the GRS, a substantial reduction of approximately $43\,\mathrm{dB}$ is observed. While this reduction can be attributed to the effect of phase synchronization, an inspection of the directivity in Figure 3a reveals that certain regions still exhibit emissions reaching about $48\,\mathrm{dB}$; however, these regions are located differently compared to those observed in the $\Delta\phi = 0°$ case. For this reason, a less ambiguous method for evaluating the effect of noise reduction caused by the phase angle is employed by computing the SWL, as explained in Section 2.2, and by interpreting results in terms of acoustic power levels expressed in decibels. For the first BPF harmonic, values of $L_w = 85.71\,\mathrm{dB}$ and $L_w = 78.24\,\mathrm{dB}$ are obtained for the in-phase and opposite-phase cases, respectively. This corresponds to a reduction of $\Delta L_w = 7.47\,\mathrm{dB}$ in acoustic power due to the phase angle effect. Turning to the second BPF harmonics, these are shown in Figure 2b for $\Delta\phi = 0°$ and in Figure 3b for $\Delta\phi = 30°$. Unlike the first harmonic, the tonal directivity is found to be very similar and is characterized by a lobed spatial distribution that peaks along the X-axis in both cases. When the SWL is computed, values

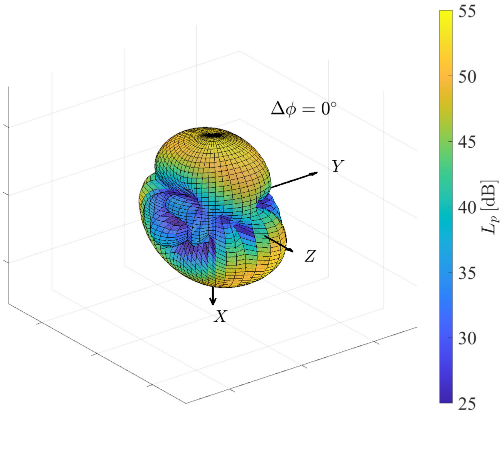

(a) 1^{st} BPF harmonic.

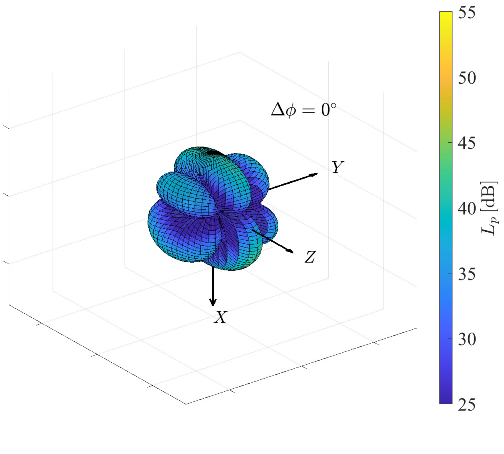

(b) 2^{nd} BPF harmonic.

Figure 2: Three-dimensional L_p directivity of the BPF harmonic tones for the $\Delta\phi = 0°$ configuation.

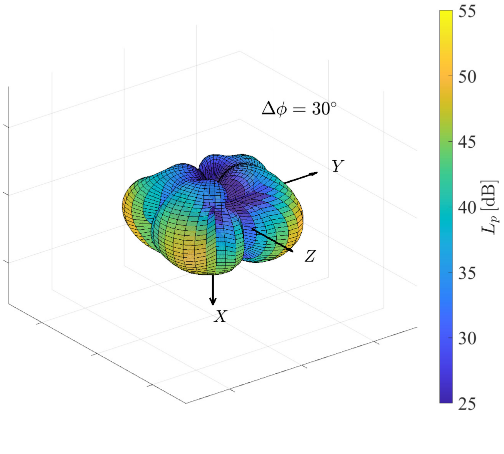

(a) 1^{st} BPF harmonic.

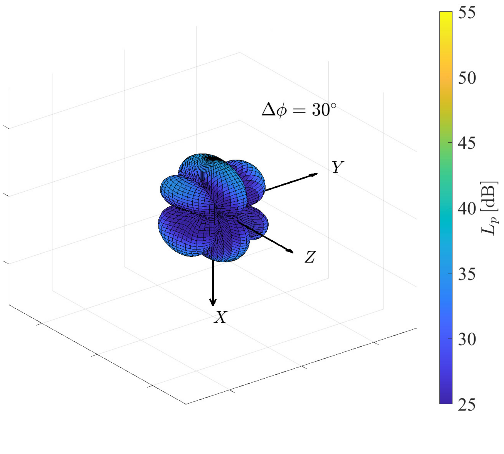

(b) 2^{nd} BPF harmonic.

Figure 3: Three-dimensional L_p directivity of the BPF harmonic tones for the $\Delta\phi = 30°$ configuration.

of $L_w = 73.76\,\text{dB}$ and $L_w = 68.97\,\text{dB}$ are obtained for the two configurations, respectively. This indicates a reduction of $\Delta L_w = 4.79\,\text{dB}$ in acoustic power due to the phase angle for the second BPF harmonic.

4. CONCLUSIONS

In recent years, significant tonal noise attenuation has been reported in several experimental studies on phase synchronization in DEP systems. However, these conclusions have often been based on discrete SPL measurements taken at isolated locations, which may not fully capture the three-dimensional nature of acoustic radiation. As a result, the spatial redirection of tonal components may have been misinterpreted as global attenuation, raising questions about the generalizability of the findings. To address this limitation, a methodology has been employed in the present study, relying on high-fidelity numerical simulations already available in the literature [12], combined with a dipole-based far-field noise formulation and a dense spherical microphone array. Through this approach, the spatially integrated SWL can be computed, providing a global and physically meaningful metric for quantifying tonal acoustic emissions. A three-propeller DEP configuration has been considered in the analysis, with a comparison made between in-phase ($\Delta\phi = 0°$) and opposite-phase ($\Delta\phi = 30°$) operation under forward-flight conditions. It has been shown that in-phase rotation produces highly directional radiation patterns at the first BPF harmonic, particularly along the X and Z axes, whereas the opposite-phase configuration yields a markedly different spatial distribution, with peak emissions occurring elsewhere. This suggests that tonal energy is drastically redistributed by phase synchronization, resulting in either mitigation or amplification depending on the spatial location considered. Nevertheless, notable reductions in SWL have been observed in the $\Delta\phi = 30°$ case, with decreases of $\Delta L_w = 7.47\,\mathrm{dB}$ in acoustic power for the first BPF harmonic and $\Delta L_w = 4.79\,\mathrm{dB}$ for the second. In future studies, a broader range of phase angles, rotor counts, and operating conditions should be explored, and hybrid strategies that combine synchronization with aerodynamic optimization should be considered for more effective and scalable noise control.

5. ACKNOWLEDGMENTS

This research was carried out within the framework of the H2020 Research and Innovation Actions ENODISE (ENabling Optimized DISruptivE airframe-propulsion integration concepts) and eVTOLUTION (eVTOL Multi-fidelity Hybrid Design and Optimization for Low Noise and High Aerodynamic Performance), both funded by the European Commission under Grant Agreement numbers 860103 and 101138209, respectively. Furthermore, the authors would like to acknowledge Prof. Daniele Ragni and Prof. Damiano Casalino from TU Delft (The Netherlands) and Prof. Francesco Avallone (Politecnico di Torino, Italy) for the inspiring discussions about aeroacoustics and computational fluid mechanics.

6. REFERENCES

[1] NASA, "Strategic implementation plan: 2017 update." `https://www.nasa.gov/sites/default/files/atoms/files/sip-2017-03-23-17-high.pdf`, 2017.

[2] A. Zarri, E. Dell'Erba, W. Munters, and C. Schram, "Aeroacoustic installation effects in multi-rotorcraft: Numerical investigations of a small-size drone model," *Aerospace Science and Technology*, vol. 128, p. 107762, 2022.

[3] H. Lee and D.-J. Lee, "Rotor interactional effects on aerodynamic and noise characteristics of a small multirotor unmanned aerial vehicle," *Physics of Fluids*, vol. 32, no. 4, 2020.

[4] K. A. Pascioni, S. A. Rizzi, and N. Schiller, "Noise reduction potential of phase control for distributed propulsion vehicles," American Institute of Aeronautics and Astronautics, 2019.

[5] M. Shao, Y. Lu, X. Xu, S. Guan, and J. Lu, "Experimental study on noise reduction of multi-rotor by phase synchronization," *Journal of Sound and Vibration*, vol. 539, p. 117199, Oct. 2022.

[6] S. Guan, Y. Lu, T. Su, and X. Xu, "Noise attenuation of quadrotor using phase synchronization method," *Aerospace Science and Technology*, vol. 118, p. 107018, 2021.

[7] B. Turhan, H. K. Jawahar, A. Gautam, S. Syed, G. Vakil, D. Rezgui, and M. Azarpeyvand, "Acoustic characteristics of phase-synchronized adjacent propellers," *The Journal of the Acoustical Society of America*, vol. 155, pp. 3242–3253, May 2024.

[8] E. De Paola, R. Camussi, G. Stoica, A. Di Marco, and G. Capobianchi, "Aerodynamic and aeroacoustic experimental investigation of a three propellers DEP configuration," *Aerospace Science and Technology*, p. 109508, 2024.

[9] M. Roger, D. Acevedo-Giraldo, and M. C. Jacob, "Acoustic versus aerodynamic installation effects on a generic propeller-driven flying architecture," *International Journal of Aeroacoustics*, vol. 21, no. 5-7, pp. 585–609, 2022.

[10] R. de Vries, N. van Arnhem, T. Sinnige, R. Vos, and L. L. Veldhuis, "Aerodynamic interaction between propellers of a distributed-propulsion system in forward flight," *Aerospace Science and Technology*, vol. 118, p. 107009, Nov. 2021.

[11] A. Zarri, A. Koutsoukos, F. Avallone, F. de Prenter, D. Ragni, and D. Casalino, "Aerodynamic and acoustic interaction effects of adjacent propellers in forward flight," *AIAA AVIATION 2023 Forum*, 2023.

[12] F. D. Prenter, A. Zarri, and D. Casalino, "Low-cost computational modeling of aeroacoustic interactions between adjacent propellers," *30th AIAA/CEAS Aeroacoustics Conference (2024)*, 2024.